

**Suppression of photocatalytic efficiency in highly N-doped anatase films**

Takeshi Okato, Tatsunori Sakano, and Minoru Obara\*

*Department of Electronics and Electrical Engineering, Keio University, 3-14-1, Hiyoshi, Kohoku-ku, Yokohama-shi, 223-8522 Japan*

(Received 5 March 2005; revised manuscript received 1 August 2005; published 29 September 2005)

We report the role of N in epitaxial films of anatase  $\text{TiO}_2$ . The films were artificially grown with a two-step temperature-tuned epitaxy which utilized the high-temperature cubic phase of  $\text{LaAlO}_3$  substrates. The preparation of highly crystallized anatase with various N concentrations ( $C_N \leq 3.85$  at. %) allowed us to identify the optimum dopant concentration ( $C_N = 1-2$  at. %). At higher doping levels, N is found to be difficult to substitute for O having been predicted to contribute to the band-gap narrowing, giving rise to the undesirable deep-level defects. In addition, a study by x-ray and Raman spectroscopy revealed that the growth of anatase became more difficult, and the stable phase was shifted to rutile at the higher N concentrations.

DOI: [10.1103/PhysRevB.72.115124](https://doi.org/10.1103/PhysRevB.72.115124)

PACS number(s): 78.20.-e, 68.55.-a, 81.15.-z, 82.50.Hp

**I. INTRODUCTION**

Photocatalysis is a generic term for surface chemical reactions resulting from photoinduced carriers. Among the well-known photocatalytic materials (e.g.,  $\text{ZnO}$ ,  $\text{CdSe}$ ,  $\text{SrTiO}_3$ , and  $\text{TiO}_2$ ),  $\text{TiO}_2$  is the most promising photocatalyst with its chemical stability, high reactivity, and low environmental pollution. The crystal phase of  $\text{TiO}_2$  is classified into three types, i.e., rutile, brookite, and anatase.<sup>1,2</sup> The anatase presents the strongest photocatalytic activity among them and is widely used for photocatalyst; nevertheless, it is a low-temperature metastable phase and it is difficult to obtain a single crystal. The most significant limitation to the application of anatase is its optical band gap. Anatase has an indirect band gap of  $\sim 3.2$  eV, and exhibits a photocatalytic activity only under ultraviolet light illumination ( $\lambda < 387$  nm). This has prompted many groups to investigate the enhancement of its photocatalytic activity under visible light illumination. In the past decades, the doping of metal ions has been recognized as a promising solution.<sup>3-5</sup> The improved photocatalytic performance is explained by the shallow charge-trapping sites produced by the cationic dopant which partially prevents the undesirable recombination of electron-hole pairs.

Sato reported sensitized photocatalytic activity under visible light illumination with a nitrogen dopant in 1986.<sup>6</sup> In 2001, Asahi *et al.* explained the effect of N doping using spin-restricted local-density-functional approximation (LDA) calculations for anatase.<sup>7</sup> They pointed out that the substitute N is effective for band-gap narrowing by mixing with the O  $2p$  state in the anatase matrix, and experimentally verified the enhanced optical absorption at less than 500 nm. Subsequently, the superiority of N-doped  $\text{TiO}_2$  is demonstrated from the viewpoint of photocatalytic activity,<sup>8-10</sup> surface hydrophilicity,<sup>11</sup> and photoinduced carrier response<sup>12</sup> under visible light illumination. However, samples with varying N-dopant concentrations have not been studied due to the difficulty of the chemically stable nitrogen doping into the metastable anatase. Therefore, there is a lack of correct understanding of the effects of N at high dopant levels. While Burda *et al.* reported the enhancement of N incorporation up to 8 at. % into anatase nanoparticles,<sup>8</sup> degraded photocata-

lytic efficiencies at a high N concentration have been predicted by Lindgren *et al.*<sup>12</sup>

For the metal doping method, it is known that the photocatalytic activity strongly depends on the doping concentration, and there exists an optimum value for each dopant. Many hypotheses have been suggested to explain the mechanism for the drawbacks at the high doping levels: (1) The higher concentration traps more electrons and/or holes, lowering the carrier mobility;<sup>13,14</sup> and (2) metal ions produce not only shallow traps but also deep-level defects which act as recombination centers.<sup>15</sup> In this paper, we will report the growth of highly textured anatase films and demonstrate the optimum N concentration for the photocatalytic efficiency. The N-doped anatase crystal was artificially grown by employing two-step temperature-tuned epitaxy. The N concentration was controlled using homemade  $\text{TiO}_{2-2x}\text{N}_x$  targets.

**II. EXPERIMENTS**

N-doped  $\text{TiO}_2$  films were grown by KrF excimer pulsed-laser deposition (PLD). The ablation targets were prepared by mixing rutile  $\text{TiO}_2$  and TiN powders in various ratios. By changing the ratio, we obtained various N concentrations ( $C_N$ ) from 0 to 30 at. % in the targets. The films were deposited on (100)  $\text{LaAlO}_3$  substrates. The substrates were heated by a standard resistive heater which was varied from 300 to 550 °C. The base pressure of the process chamber was evacuated to as low as  $10^{-4}$  Pa, and then it was back-filled with oxygen to  $10^{-1}$  Pa. A deposition run was performed for 30 min and a deposition rate of 20 nm  $\text{min}^{-1}$  was achieved. To obtain information about the N states, x-ray photoelectron spectroscopy (XPS, 9000-MC, JEOL) was carried out. The structural characteristics of the thin films were determined by x-ray diffraction (XRD, RAD-C, Rigaku) and a Raman spectrometer (CCD-Raman-One, Chromex). The photocatalytic activity was evaluated by measuring the decomposition of a methylene blue solution (15 ppm).

**III. RESULTS AND DISCUSSION****A. Two-step temperature-tuned epitaxy of N-doped anatase films**

It is well known that the crystal structure of  $\text{LaAlO}_3$  undergoes crystallographic transitions by changing the tem-

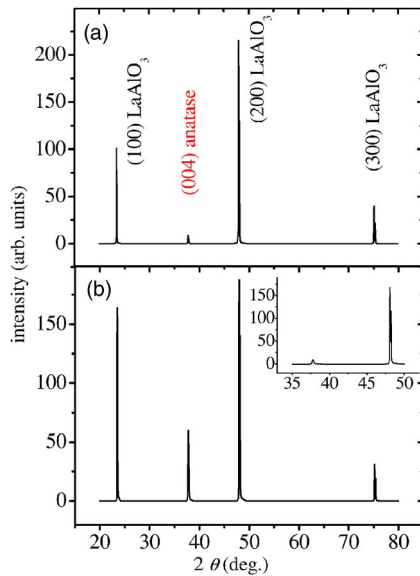


FIG. 1. (Color online)  $2\theta$ - $\theta$  XRD scans of  $\text{TiO}_2$  films grown using an undoped  $\text{TiO}_2$  target at (a) 500 °C and (b) 300 °C with a high-temperature buffer layer. The inset in (b) is the scan around the (004) anatase peak of the HTBL grown at 550 °C for 5 min.

perature. A gradual change from a rhombohedral to high-temperature cubic structure was observed by Geller and Bala.<sup>16</sup> They pointed out that the critical temperature ( $T_c$ ) was 435 °C. However, this  $T_c$  was not correctly measured. Nowadays, there are many reports concerning the  $T_c$  of  $\text{LaAlO}_3$ ; however, this is beyond the current scope of this paper. The generally accepted transition temperature ranges between 530 and 550 °C.<sup>17</sup> Since the lattice mismatch between the cubic  $\text{LaAlO}_3$  and anatase is very small ( $\sim 0.2\%$ ), epitaxy in the high-temperature phase is absolutely necessary. It is expected that the crystallographic structure of the deposited films dramatically changes around  $T_c$ . In our study, while a clear anatase peak was easily obtained at 550 °C, the films grown below 400 °C did not indicate any XRD peaks.

Figure 1(a) shows the XRD spectrum of the film grown at 500 °C using an undoped  $\text{TiO}_2$  target. The shallow anatase diffraction peak suggests the incomplete transition of  $\text{LaAlO}_3$ . At the same time, we must avoid the oxidation of the Ti-N bond by the *in situ* thermal annealing. Hsieh *et al.* observed the dependence of the film oxidation on the annealing temperature using TiN films grown on  $\text{SrTiO}_3$  substrates.<sup>18</sup> They found that the TiN was easily oxidized and fully disappeared at 600 °C. Figure 2(c) shows the N 1s core levels investigated with XPS for the film grown at 500 °C using a  $C_N=30$  at. % target. As can be seen in Fig. 2(c), there is only a shallow peak from N (400 eV), suggesting that most of the TiN suffers from oxidation during the growth.

It is now clear that the anatase films are obtainable above the  $T_c$  at the expense of the N doping. To circumvent this dilemma, we developed the two-step temperature-tuned epitaxy, which used a high-temperature buffer layer (HTBL) as a nucleation layer of the anatase. The HTBL was prepared at 550 °C for 5 min. The substrate temperature was then decreased to the desired temperature. Figure 1(b) shows the

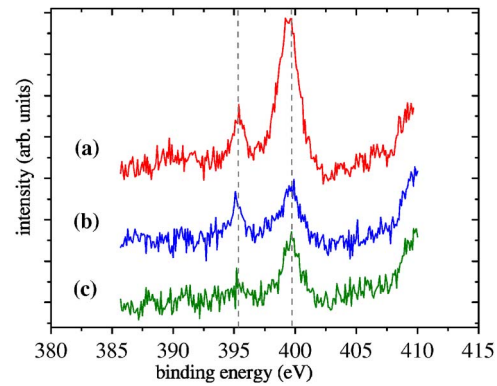


FIG. 2. (Color online) Differences in N 1s core-level XPS spectra of N-doped  $\text{TiO}_2$  films grown at various conditions. (a) and (b) are grown at 300 °C with a HTBL using  $C_N=30$  at. % and 5 at. % target, respectively. (c) is grown at 500 °C using  $C_N=30$  at. % target without a HTBL.

XRD spectrum of the film grown at 300 °C with HTBL using an undoped  $\text{TiO}_2$  target. A clear anatase peak is observable, which was not possible without the buffer layer at such a low temperature. The inset in Fig. 1(b) is a typical XRD spectrum of a buffer layer. As the nucleation layer is very thin, the diffraction peak is very shallow. Based on these figures, it is obvious that the diffraction peak seen in Fig. 1(b) is not from the buffer layer. It should be noted that even when we used a highly N-doped target (up to 30 at. %), we exclusively obtained a single oriented (004) anatase peak and no persisting TiN phases. The XPS spectrum of the N-doped  $\text{TiO}_2$  film grown at 300 °C with the HTBL using a  $C_N=30$  at. % target is illustrated in Fig. 2(a). It is clearly seen that the peak from N is dramatically increased compared to Fig. 2(c). The calculated  $C_N$  in the films and full width at half maximum (FWHM) of (004) anatase peaks are summarized in Table I.

Figures 2(a) and 2(b) show the N states in the lattice with different dopant concentrations prepared using  $C_N=30$  and 5 at. % targets. These spectra represent two differential peaks of N centered at 396 and 400 eV. The lower-energy peak corresponds to Ti-N bonding, as observed by Saha and Tompkins.<sup>19</sup> They also assigned the peaks of 400 and 402 eV to molecularly chemisorbed  $\text{N}_2$ . Indeed, the clear peaks at 402 and 400 eV were observed from TiON synthesized through TiN oxidation or  $\text{TiO}_2$  nitridation.<sup>7,19</sup> However, the 402 eV peak was hardly seen from the TiON films grown by sputtering or PLD, not only in this study but in previous reports.<sup>9,11</sup> Here, we believe that the 402 eV peak results from moleculelike  $\text{N}_2$ , which is confined under the oxide layer or literally adsorbed on the surface (or just below) during the TiN oxidation or  $\text{TiO}_2$  nitridation process. Also, it is reasonable to consider that  $\text{N}_2$  evaporates during thin-film growth processes, especially when they are performed in a vacuum chamber at high temperatures. Taking into account that the TiAlN film XPS peaks appeared at 403.2 eV and no other peak was observed above 398 eV,<sup>20</sup> the N 1s peak at 400 eV is likely newly created by oxygen, and it should be interpreted as the Ti-O-N oxynitride. This discussion is well consistent with recent silicon oxynitride studies.<sup>21,22</sup> But,

TABLE I. Dependence of N-dopant concentration ( $C_N$ ) on the film characteristics for anatase samples grown on HTBL/(100)LaAlO<sub>3</sub> substrates at 300 °C.

$C_N$ in target (at. %)	$C_N$ in film (at. %)	FWHM of XRD for anatase (deg)	Redshift denoted by $\Delta E_g$ (eV)	Remaining $C_{MB}$ after the irradiation (ppm)	
				uv	VIS
0		0.167		3.01	7.42
2	<1	0.171	0.072	1.77	7.28
5	1.28	0.178	0.094	1.21	6.41
10	1.69	0.180	0.090	0.907	6.55
20	2.55	0.179	0.099	2.06	6.59
30	3.85	0.374	0.107	3.03	6.43

even if we cannot detect a N<sub>2</sub> signal, it does not mean there is no moleculelike N<sub>2</sub>, since a small quantity of it may be embedded below the XPS detection limit.<sup>21</sup> Indeed, interstitially doped N (N<sub>i</sub>) can make a N<sub>2</sub> bond with substitutional N (N<sub>O</sub>) at high doping levels in a N-doped metal oxide.<sup>23</sup>

According to Ref. 7, the replacement of the O atom with N is effective for band-gap narrowing, while the interstitial ones in the anatase matrix produce deep-level defects in the band gap. Therefore, the increment of N<sub>i</sub> is unfavorable. Provided that N atoms substitute at O sites, both 397 eV(Ti-N) and 400 eV(Ti-O-N) peaks should simultaneously increase. However, the peak at 400 eV is highlighted along with the  $C_N$ , while the 397 eV peak remains unchanged, as can be seen in Fig. 2. This implies that the doping into the desired site (N<sub>O</sub>) is saturated at low dopant levels, and the excess of N is doped interstitially within the matrix. In addition, it is worth pointing out that the anatase growth at a low temperature has a significant importance for the substitutionally doped impurity due to the structural instabilities at high temperatures.<sup>24</sup> In the case of N, the formation of a Ti-O bond is energetically favorable compared with that of Ti-N. The film grown at 500 °C [Fig. 2(c)] does not indicate the spectrum of the Ti-N bond, suggesting the formation of N<sub>i</sub> defects resulting from O atoms which fill the appropriate sites by pushing aside the N<sub>O</sub> during the annealing process at such a high temperature. This result is reasonable considering the differential formation enthalpy of  $\Delta H_f = -938.7$  kJ mol<sup>-1</sup> for anatase and  $-337.9$  kJ mol<sup>-1</sup> for TiN.

**B. Properties of the N-doped anatase films**

Figure 3(a) shows the photographs of as-grown N-doped anatase epilayers with various N concentrations. The color of the film changed from transparent to yellowish along with the change in the N concentration, indicating that the absorption of visible light is enhanced, which corresponds well with other reports.<sup>6-12</sup> However, the effect of the N dopant should be determined with caution. Nevertheless, heavily N-doped films certainly show highly enhanced optical absorption; the redshifts in the absorption edge ( $\Delta E_g$ ) are less affected by the increased  $C_N$ . The absorption edge of the N-doped anatase films is presented in Fig. 3(b). These spectra are significantly affected by the Burstein shift and band-

tailing effect especially when N is heavily doped. The optical transmission of the N-doped film grown from a  $C_N = 30$  at. % target [lower right in Fig. 3(a)] gradually increases up to 500–550 nm; however, it is still less than half of the undoped TiO<sub>2</sub> film in the whole visible spectrum. The remarkable feature seen in Fig. 3(b) is that the visible light is transmitted when it is longer than 380 nm, indicating that the band-gap narrowing has hardly occurred. The inset in Fig. 3(b) shows the estimated optical band gap from these curves. The observed redshifts of the absorption edges from the undoped film are also presented in Table I. The small quantity of N seems to narrow the band gap, even though it is only by 0.07 eV. However, with an increase of  $C_N$ , it is clearly seen that the band gap hardly became any narrower. The highly doped film ( $C_N=3.85$  at. %) has a downward shift of only

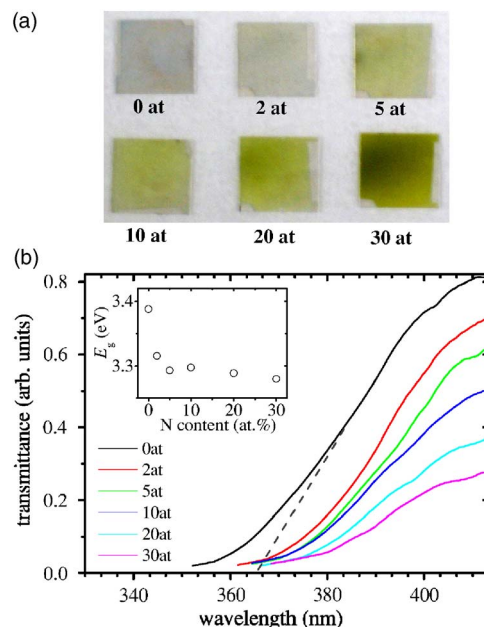


FIG. 3. (Color online) (a) Photographs of N-doped anatase epilayers. The  $C_N$  of ablation targets used are indicated below the respective specimens. (b)  $C_N$  dependence of absorption edges of N-doped anatase epilayers. The curves from left to right correspond to those of the samples grown from  $C_N=0, 2, 5, 10, 20,$  and  $30$  at. % targets. The redshift of the band gap ( $E_g$ ) is plotted in the inset.



$\sim 0.04$  eV compared with the film containing the lowest  $C_N$ . Therefore, the absorption and photocatalytic activity produced by the visible light ( $\lambda=400\text{--}550$  nm) likely originate from the N-related visible light absorptive defects, rather than a band-to-band transition within a narrowed band gap. Such discussion is consistent with recent papers.<sup>10–12,25</sup>

Taking into account the XPS results, the saturation of band-gap shift and the film coloring likely originate from  $N_O$  and  $N_i$ , respectively. The absorption of the visible light ( $\lambda > 400$  nm) is merely caused by the deep-level defects, so that the optimum  $C_N$  should be more pronounced. Recently, Nakano *et al.* reported the defect created by nitrogen in N-doped anatase film deposited on  $n^+$ -GaN/ $Al_2O_3$  substrates.<sup>26</sup> They point out that a deep-level defect located at 2.48 eV below the conduction band is introduced by N. Although it is hard to conclude that this deep-level defect contributes to the band-gap narrowing according to the above discussion, it is very important to determine the effect of this defect. To investigate the photocatalytic activity of N-doped films, we have used both uv and visible light illumination. The uv light source applied is a commercial black light (EFD15BLB, Toshiba) which emits long-wavelength uv rays centered on 352 nm, where wavelengths below 320 nm and visible light from the Hg lamp are cut by the filter. The visible light (hereafter VIS) source is a blue-light-emitting diode (LED E1L55-7B0A, Toyoda Gosei) centered on 475 nm ( $\sim 2.6$  eV) with a photon energy slightly higher than the N-related defects (2.48 eV) and well lower than the optical band gap of N-doped anatase.

The concentration of methylene blue ( $C_{MB}$ ) after a 36-h uv illumination is summarized in Table I. As can be clearly seen in Table I, there is a strong correlation with  $C_N$ . We found that the photocatalytic activity was enhanced under ultraviolet illumination owing to the N doping at low  $C_N$ , and it reached the highest decomposition efficiency at  $C_N = 1.69$  at. %. The enhancement is explained by the small band-gap shift (resulting from  $N_O$ ) and charge-trapping sites ( $N_i$ ), which raise the efficiency of electron-hole generation and prevent undesirable recombination. The degraded photocatalytic efficiency at the high dopant levels is reasonable considering the interfusions of excessive  $N_i$  defects, which can lower the carrier mobility and act as recombination centers. The  $C_{MB}$  after a 72-h VIS illumination is summarized in Table I, as well. Here, we also find that the decomposition rate of the N-doped  $TiO_2$  is enhanced. The improved efficiency originates from visible light absorptive defects considering the photon energy of the LED light. The decomposition from the undoped  $TiO_2$  sample is likely caused by defect levels within the band gap or direct photodecomposition of methylene blue. Here, we have to note the degree of enhancement through N doping is not significant compared to the uv irradiation experiment. More importantly, the decomposition rate is not strongly affected by the  $C_N$  in the film when it is larger than 1 at. %. The improvement up to 1 at. % is reasonable, since the optical absorption is enhanced by N, as can be seen in Fig. 3(a). Considering the use of N-doped  $TiO_2$  under solar light or fluorescence light, where both contain a small amount of uv light, N doping is still very attractive, since it can benefit from the visible and

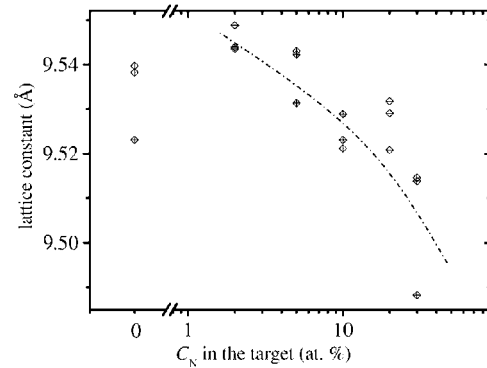


FIG. 4.  $C_N$  dependence of the lattice distortion represented by the  $c$ -axis length. The dashed line is a guide indicating the possible behavior as a function of the  $C_N$ .

uv spectra. Here, we point out that  $C_N$  of 1–2 % is the optimum concentration for practical applications, and more N is not necessary; more N turns colorless  $TiO_2$  yellowish and degrades its efficiency.

Another finding of the adverse impact of  $N_i$  is on the crystallographic structure. For the anatase polymorph, the structural variation following the replacement of one O atom with N in the anatase is less pronounced, because Ti-N bond lengths (1.964 and 2.081 Å) are only slightly longer than the Ti-O ones (1.942 and 2.002 Å) in the matrix.<sup>25</sup> Therefore, N incorporation at an O site may not degrade the crystallinity. A small concentration of N even promotes the growth of anatase, as reported by Lindgren *et al.*<sup>12</sup> However, it is controversial at high dopant levels. Figure 4 shows the distortion of the lattice constant represented by the  $c$ -axis lengths as a function of  $C_N$  in the ablation target. The errors correspond to the dispersion of the data for different films grown under the same conditions or to the experimental error in the determination of the lattice constant by XRD. The lattice was expanded by N incorporation at  $C_N=2$  at. %; however, it decreases with further increments of  $C_N$ . The first expansion originates from the replacement of the Ti-O bonds with Ti-N ones. The following shrinkage behavior suggests that the amount of  $N_i$  is increasing, as the lattice is compressed by the interstitial dopant. At the same time, the  $N_i$  inside the anatase elevates the density of the  $TiO_2$  matrix by their volume, which may act as a driving force of the structural phase transformations.<sup>27</sup> For instance, the density of rutile (4.25 g  $cm^{-3}$ ) is higher than that of anatase (3.89 g  $cm^{-3}$ ).

To elucidate the dominant growth mode with various N concentrations, we have grown films on amorphous  $SiO_2$  substrates at 300 °C. There is no epitaxial relationship here, and films can grow free from the influence of substrates. Figure 5 shows the Raman shift of the films, where  $C_N =$  (a) 2, (b) 10, and (c) 30 at. % targets were used, respectively. In Fig. 5, the peaks of the 442 and 610  $cm^{-1}$  bands marked with  $R$  indicate the existence of the rutile phase, while the 399, 520, and 643  $cm^{-1}$  bands marked with  $A$  are the anatase ones.<sup>28</sup> The film deposited at a low dopant concentration clearly exhibits the anatase spectra partially mixed with the rutile modes. With increasing  $C_N$ , the characteristic band of anatase at 520  $cm^{-1}$  is weakened. Also, the anatase peaks of 399 and 643  $cm^{-1}$  are gradually shifting toward the

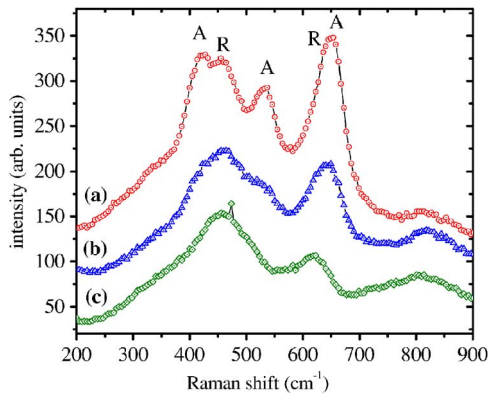


FIG. 5. (Color online) Raman spectra of the as-grown N-doped  $\text{TiO}_2$  films on amorphous  $\text{SiO}_2$  substrates with various  $C_N$ : (a) 2, (b) 10, and (c) 30 at. %. The Raman shifts from rutile and anatase are indicated by R and A, respectively.

rutile peaks of  $442$  and  $610\text{ cm}^{-1}$ , respectively. These results reveal that the amount of the rutile phase increases at the higher dopant levels, indicating that the growth of anatase becomes more difficult. This is consistent with the broadened FWHM of the XRD spectra of the anatase as shown in Table I. The superiority of the photocatalytic activity using the anatase phase is claimed elsewhere. Moreover, the blueshift in the absorption edge is pointed out in the N-doped rutile  $\text{TiO}_2$ .<sup>25,29</sup> This observation also explains the origin of drawbacks, in addition to the N-related defect formation at high N-doping levels.

The difficulty imposed upon realizing higher photocatalytic efficiency and/or band-gap narrowing in anatase is the existence of large amounts of  $N_i$ , because the N that is effective for them is not  $N_i$  but  $N_O$ . Actually, at lower concentrations, the substitute N does not cause band-gap narrowing, and the N  $2p$  states are localized just above the O  $2p$  valence band as recently proven by Valentin *et al.*<sup>25</sup> In this regard, only a small redshift of  $E_g$  obtained in this work is reasonable. The theoretical prediction for the band-gap narrowing calculated by Asahi *et al.* was modeled by replacing an O atom with N in the 16 atom of O in the unit cell of anatase, producing an  $\sim 4.2$  at. %  $N_O$  doping;<sup>7</sup> however, such a high substitutional doping level is unrealistic in our work. This observation leads to the question as to whether a further

band-gap narrowing occurs. Our results clearly indicate that  $N_O$  is saturated at low dopant levels, and there exists a large amount of  $N_i$  at high dopant levels. However, the possibility remains that one could obtain a further redshift of the absorption edge, if the amount of  $N_O$  were successfully increased, for instance, through low-temperature nonequilibrium growth conditions.

#### IV. SUMMARY

We have given microscopic insights into the nature of the photocatalytic N-doped anatase films. The N-doped epitaxial anatase films were artificially prepared by employing a high-temperature buffer layer as nucleation layer. This technique enabled anatase growth even at a temperature lower than the crystallographic transition of  $\text{LaAlO}_3$ , and led to the enrichment of N up to 3.85 at. %. The transparent film color gradually turns to yellowish as  $C_N$  increases, indicating that the optical absorption is enhanced. However, the optical band-gap narrowing effect anticipated by N doping did not occur with the increment of  $C_N$ . This is explained by the saturation of N doping into O sites, and the excessive N is interstitially doped within the matrix to produce deep-level defects. When these films are exposed to uv light, the efficiency is strongly affected by  $C_N$ . At low dopant concentrations, the photocatalytic decomposition rate was improved, and it reached the highest value near  $C_N=1.7$  at. %. Here, the existence of the optimum value is explained by the slight redshift of the band gap and visible light absorptive  $N_i$  defects which degrade the efficiency when there are too many. On the contrary, in the case of VIS light, the efficiency is less affected by  $C_N$ , especially when it is larger than 1 at. %. In addition, the study of x-ray and Raman spectroscopy revealed that the growth of anatase became rather difficult, and the stable phase was rutile at higher N concentrations. These observations lead us to conclude that optimum  $C_N$  is 1–2 at. % provided that TiON is grown under typical conditions.

#### ACKNOWLEDGMENTS

This work was supported in part by a Grant-in-Aid for Scientific Research (Grant No. A15206011) from MEXT in Japan. T.O. is grateful to JSPS for financial support.

\*Electronic address: obara@obara.elec.keio.ac.jp

- <sup>1</sup>S.-D. Mo and W. Y. Ching, *Phys. Rev. B* **51**, 13023 (1995).
- <sup>2</sup>R. Asahi, Y. Taga, W. Mannstadt, and A. J. Freeman, *Phys. Rev. B* **61**, 7459 (2000).
- <sup>3</sup>W. Choi, A. Termin, and M. R. Hoffman, *J. Phys. Chem.* **98**, 13669 (1994).
- <sup>4</sup>M. I. Litter and J. A. Navio, *J. Photochem. Photobiol., A* **98**, 171 (1996).
- <sup>5</sup>D. Morris, R. Dixon, F. H. Jones, Y. Dou, R. G. Egdell, S. W. Downes, and G. Beamson, *Phys. Rev. B* **55**, 16083 (1997).
- <sup>6</sup>S. Sato, *Chem. Phys. Lett.* **123**, 126 (1986).

- <sup>7</sup>R. Asahi, T. Morikawa, T. Ohwaki, K. Aoki, and Y. Taga, *Science* **293**, 269 (2001).
- <sup>8</sup>C. Burda, L. Yongbing, C. Xiaobo, A. C. S. Samia, J. Stout, and J. L. Gole, *Nano Lett.* **3**, 1049 (2003).
- <sup>9</sup>Y. Suda, H. Kawasaki, T. Ueda, and T. Ohshima, *Thin Solid Films* **453-454**, 162 (2004).
- <sup>10</sup>S. Sakthivel and H. Kisch, *ChemPhysChem* **4**, 487 (2003).
- <sup>11</sup>H. Irie, S. Washizuka, N. Yoshino, and K. Hashimoto, *Chem. Commun. (Cambridge)* **11**, 1298 (2003).
- <sup>12</sup>T. Lindgren, J. M. Mwabora, E. Avendano, J. Jonsson, A. Hoel, C.-G. Granqvist, and S.-E. Lindquist, *J. Phys. Chem. B* **107**,

- 5709 (2003).
- <sup>13</sup>Z. Zhang, C.-C. Wang, R. Zakaria, and J. Y. Ying, *J. Phys. Chem. B* **102**, 10871 (1998).
- <sup>14</sup>V. Kytin, Th. Dittrich, J. Bisquert, E. A. Lebedev, and F. Koch, *Phys. Rev. B* **68**, 195308 (2003).
- <sup>15</sup>T. Miyagi, M. Kamei, I. Sakaguchi, T. Mitsuhashi, and A. Yamazaki, *Jpn. J. Appl. Phys., Part 1* **43**, 775 (2004).
- <sup>16</sup>S. Geller and V. V. Bala, *Acta Crystallogr.* **9**, 1019 (1956).
- <sup>17</sup>See, for example, S. Geller and P. M. Raccach, *Phys. Rev. B* **2**, 1167 (1970).
- <sup>18</sup>C. C. Hseih, K. H. Wu, J. Y. Juang, T. M. Uen, J.-Y. Lin, and Y. S. Gou, *J. Appl. Phys.* **92**, 2518 (2002).
- <sup>19</sup>N. C. Saha and H. G. Tompkins, *J. Appl. Phys.* **72**, 3072 (1992).
- <sup>20</sup>F. Esaka, K. Furuya, H. Shimada, M. Imamura, N. Matsubayashi, T. Sato, A. Nishijima, T. Kikuchi, A. Kawana, and H. Ichimura, *Surf. Sci.* **377–379**, 197 (1997).
- <sup>21</sup>H. J. Song, H. J. Shin, Y. Chung, J. C. Lee, and M. K. Lee, *J. Appl. Phys.* **97**, 113711 (2005).
- <sup>22</sup>G. F. Cerofolini, A. P. Caricato, L. Meda, N. Re, and A. Sgamellotti, *Phys. Rev. B* **61**, 14157 (2000).
- <sup>23</sup>E.-C. Lee, Y.-S. Kim, Y.-G. Jin, and K. J. Chang, *Phys. Rev. B* **64**, 085120 (2001).
- <sup>24</sup>D. H. Kim, J. S. Yang, Y. S. Kim, T. W. Noh, S. D. Bu, S.-I. Baik, Y.-W. Kim, Y. D. Park, S. J. Pearton, J.-Y. Kim, J.-H. Park, H.-J. Lin, C. T. Chen, and Y. J. Song, *Phys. Rev. B* **71**, 014440 (2005).
- <sup>25</sup>C. Di Valentin, G. Pacchioni, and A. Selloni, *Phys. Rev. B* **70**, 085116 (2004).
- <sup>26</sup>Y. Nakano, T. Morikawa, T. Ohwaki, and Y. Taga, *Appl. Phys. Lett.* **86**, 132104 (2005).
- <sup>27</sup>J. Muscat, V. Swamy, and N. M. Harrison, *Phys. Rev. B* **65**, 224112 (2002).
- <sup>28</sup>T. Yamaki, T. Sumita, S. Yamamoto, and A. Miyashita, *J. Cryst. Growth* **237–239**, 574 (2002).
- <sup>29</sup>O. Diwald, T. L. Thompson, Ed. G. Goralski, S. D. Walck, and J. T. Yates, Jr., *J. Phys. Chem. B* **108**, 52 (2004).